Influence of Cr doping on the magnetic structure of the FeAs-strips compound $CaFe_4As_3$: A single-crystal neutron diffraction study

P. Manuel,[1] L. C. Chapon,[1,2] G. Trimarchi,[3] I. S. Todorov,[4] D. Y. Chung,[4] B. Ouladdiaf,[2] M. J. Gutmann,[1] A. J. Freeman,[3] and M. G. Kanatzidis[4,5]

[1]*ISIS facility, STFC Rutherford Appleton Laboratory, Chilton, Didcot, Oxfordshire OX11 0QX, United Kingdom*
[2]*Institut Laue-Langevin, 6 Rue Jules Horowitz, BP 156, 38042 Grenoble Cedex 9, France*
[3]*Department of Physics and Astronomy, Northwestern University, Evanston, Illinois 60208, USA*
[4]*Materials Science Division, Argonne National Laboratory, Argonne, Illinois 60439, USA*
[5]*Department of Chemistry, Northwestern University, Evanston, Illinois 60208, USA*

(Received 14 June 2013; revised manuscript received 12 August 2013; published 17 September 2013)

We have studied the magnetic structure of a Cr-doped iron-arsenide compound $CaFe_4As_3$ by means of single crystal neutron diffraction. The neutron data reveal that below 90 K, an antiferromagnetic structure with propagation vector $k = 0$ is adopted. Refinement of the magnetic structure using one of the modes allowed by symmetry analysis indicates that two of the four Fe sites, including the one where the selective substitution Fe/Cr happens, bear reduced magnetic moments. Density functional theory calculations confirm the stability of such a magnetic arrangement.

DOI: 10.1103/PhysRevB.88.104414 PACS number(s): 75.10.−b, 75.25.−j

High temperature superconductivity (SC) research was given a recent boost following the discovery of superconductivity at 26 K in noncopper based materials.[1] Perhaps the most striking similarity between these new iron-based layered compounds, such as $La[O_{1-x}F_x]FeAs$, and the high temperature cuprate (HTC) superconductors is the presence of square planar (Fe_2As_2 or CuO_2) superconducting layers. By contrast, the nature of the parent compounds, which can be tuned towards SC by doping,[2,3] or by applying pressure, is very different for the new iron arsenide and the HTC superconductors: the former are spin density wave (SDW) metals while the latter are insulators. Clearly, the ability to change the topology of the Fe_2As_2 layers and to perturb the SDW state is important to understand the electronic correlations in the new pnictides. These effects can be both realized in $CaFe_4As_3$ where, instead of forming infinite layers, the FeAs are arranged in strips along b connected in a rectangular cross pattern,[4] as shown in Fig. 1, and where Cr doping affects the SDW state.

The undoped nonsuperconducting systems, including the 122 compounds AFe_2As_2 (where A = Ba,Sr,Ca), evolve from a tetragonal to an orthorhombic structure and eventually order magnetically with commensurate antiferromagnetic (AFM) structure, bearing ordered moments less than $1\mu_B$.[5] For $CaFe_4As_3$ two transitions at $T_{N1} \approx 90$ and $T_{N2} \approx 26$ K are seen in magnetic susceptibility data,[4,6] heat capacity measurements,[6] and recent Hall effect, thermopower measurements and Mössbauer spectroscopy.[7–9] In a previous publication[10] on a powder sample of $CaFe_4As_3$ we identified the second order transition at T_{N1} with an incommensurate (ICM) longitudinal spin-density wave along the b axis with propagation vector $k = (0,\delta,0)$ and $0.375 < \delta < 0.39$ and the transition at T_{N2} with a locking into a commensurate (CM) state with $\delta = \frac{3}{8}$ where the moments remained predominantly aligned along the b axis. A later single crystal study[11] refined the low temperature commensurate structure by mixing two irreducible representations, revealing the existence of a small additional component in the ac plane.

A profound effect on the magnetic properties of $CaFe_4As_3$ can be obtained by both chemical doping and pressure.[12,13] For both hydrostatic pressure and P/Yb doping on the nonmagnetic As/Ca sites, the SDW and the ICM-CM transitions appear to be preserved; this is also the case for Cu-doping on the Fe sites.[13] By contrast doping on the magnetic Fe sites by either Co or Cr retains the higher transition temperature but suppresses the ICM-CM transition although in the former case, a third transition only visible in the derivative of the magnetization appears. These studies point towards a fairly robust SDW order. To date there has not been any magnetic structure determination on any of these doped compounds. In this paper, we report on the magnetic structure of $CaCr_{0.86}Fe_{3.14}As_3$ determined by single crystal neutron diffraction.

Neutron experiments were performed at the Institut Laue Langevin (ILL) on a needle shape single crystal of $CaCr_{0.86}Fe_{3.14}As_3$. A tin flux grown sample ($12 \times 1 \times 1$ mm) was prealigned using the OrientExpress facility and placed in a cryostat on the new neutron Laue diffractometer CYCLOPS.[14] This allowed us to quickly survey a very large portion of reciprocal space and thereby identify the magnetic propagation vector before a more quantitative study on a conventional four-circle diffractometer (D10, ILL) using the same sample, as well as to perform a rapid temperature dependence. The D10 data were collected with an incident neutron wavelength of $\lambda = 2.36$ Å by using an 80 mm^2 two-dimensional microstrip detector and normalized by monitor. Integration of the Bragg peaks was obtained by a two stage process using the program RACER (ILL). Initially, a library was built by fitting ellipsoidal shapes to a set of strong reflections (with intensities five times higher than the background). The integration of all reflections was then obtained in a second pass using this library. For each data set, the list of integrated intensities obtained was corrected for Lorentz factors and normalized to the monitor count. A set of 186 independent reflections, measured at 150 K, was used to refine the nuclear structure in the paramagnetic phase. To refine the magnetic structure, 212 independent reflections were collected at 2 K. For both data sets, removing the (020)

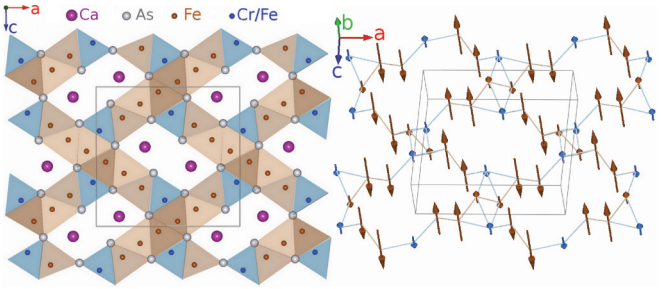

FIG. 1. (Color online) Crystal (left) and magnetic (right) structures of $CaCr_{0.86}Fe_{3.14}As_3$ at 1.5 K. The (Fe/Cr)As polyhedra, with the four (4*c*) Fe or Cr sites sitting in the middle, have been drawn to highlight the ribbon nature of the structure.

reflection considerably improved the refinements by reducing the extinction effect due to the needle shape of the sample growing along the *b* direction. Refinement of both the nuclear and magnetic structures was carried out using the FullProf program[15] and symmetry (representation) analysis is presented using Kovalev's notation.[16]

Refinements in the paramagnetic phase, collected at 150 K and consistent with a previous report,[12] indicate that the structure crystallizes in the orthorhombic space group *Pnma* with $a = 12.16(1)$, $b = 3.766(4)$, and $c = 11.80(1)$ Å. The refinement gives $R_{\text{Bragg}} = 3.39\%$ and the positions $(x, \frac{1}{4}, z)$ of the four independent (4*c*) Fe sites in the crystallographic unit cell are given in Table I. The (4*c*) sites 2, 3, and 4 are fully occupied while Cr substitutes on site 1 with a refined occupancy of 85.6(6)% comparable with the 84% obtained on a previous sample.[12]

We now turn our attention to the low temperature (1.5 K) magnetic structure. As can be seen immediately from Fig. 2, the magnetic structure is commensurate with $k = 0$ in contrast with the parent compound $CaFe_4As_3$. The decomposition of the magnetic representation for the (4*c*) sites is given by

$$\tau_{\text{mag}}(4c) = \tau_1 + 2\tau_2 + 2\tau_3 + \tau_4 + \tau_5 + 2\tau_6 + 2\tau_7 + \tau_8.$$

All the irreducible representations (irreps) are one dimensional. The τ_2, τ_3, τ_6, and τ_7 irreps correspond to ordering in the *ac* plane which is not consistent with the susceptibility.[12]

TABLE I. Amplitude of the magnetic moments (M_i) and relative phases (Φ_i) where appropriate for the four inequivalent Fe sites (i = 1–4) extracted from the refinements at 1.5 K for $CaCr_{0.86}Fe_{3.14}As_3$ (left) and for $CaFe_4As_3$ (right) from Ref. 10.

		Doped 1.5K	Undoped 30 K/1.5 K	
Site i	Position	$M_i(\mu_B)$	$M_i(\mu_B)$	Φ_i
Fe_1	$x = 0.0215(4)$	−0.48(6)	2.14(13)/	0/
	$z = 0.3141(4)$		1.4(11)	0
Fe_2	$x = 0.0661(2)$	0.46(5)	1.55(16)/	0.13(2)/
	$z = 0.5383(2)$		1.61(14)	0.14(3)
Fe_3	$x = 0.3051(2)$	1.71(5)	1.83(8)/	0.56(4)/
	$z = 0.1221(2)$		1.67(20)	0.45(3)
Fe_4	$x = 0.3155(2)$	1.58(5)	1.94(10)/	0.10(4)/
	$z = 0.7231(2)$		1.84(10)	0.01(4)

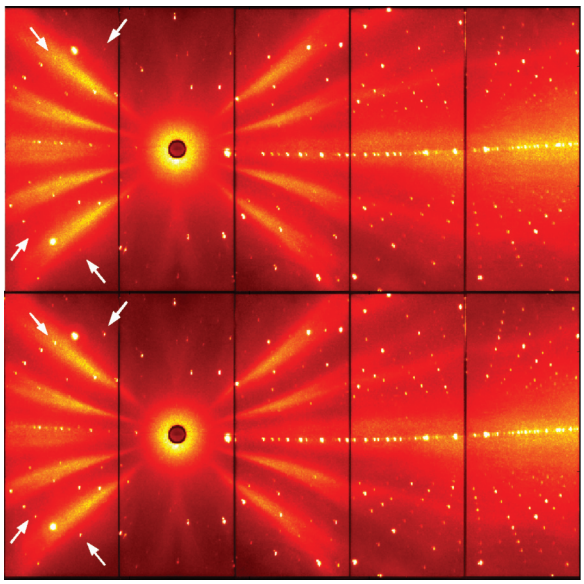

FIG. 2. (Color online) Neutron Laue patterns obtained on CYCLOPS. For both patterns, the horizontal coverage is 225° and the vertical coverage is 90°. Top: In the paramagnetic regime at 200 K. Bottom: In the magnetically ordered state at 1.5 K. The arrows highlight four peaks with strong intensities in the low temperature data and which can all be indexed with $k = 0$.

For each of the four (4*c*) sites, the moment directions for the atomic positions $(x,1/4,z), (-x,3/4,-z), (-x+1/2,3/4,z+1/2)$, and $(x+1/2,1/4,-z+1/2)$ along the *b* axis of the remaining four irreps are arranged as follows: $++--$ for τ_1, $+-+-$ for τ_4, $++++$ for τ_5, and $+--+$ for τ_8. Using Bertaut's well known notation,[17] this sequence can be rewritten as C_y, G_y, F_y, and A_y. Refinement of the low temperature data very clearly favors τ_4 with the R_f factor being two to three times better and χ^2 a factor 7 to 9 times better. This corresponds to the magnetic space group $Pn'ma$. The final refinement, with the moments on site 1 tied for the Cr and Fe, is presented in Fig. 3 and gives $R_f = 3.92\%$. Moment

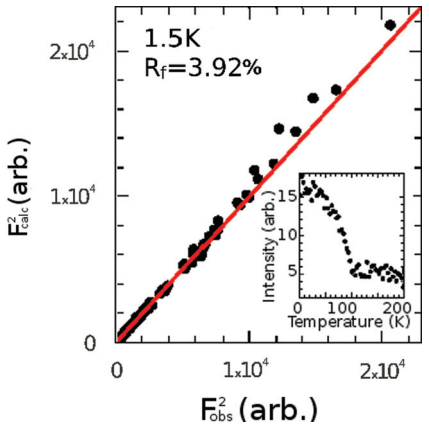

FIG. 3. (Color online) Experimental (data from D10) versus calculated structure factors for $CaCr_{0.86}Fe_{3.14}As_3$ at 1.5 K. The tight distribution of black dots around the red line $F^2_{\text{obs}} = F^2_{\text{calc}}$ indicates the high quality of the refinement. Inset: Temperature dependence of (310) peak, obtained from CYCLOPS.

values extracted from the refinement are presented in Table I. Interestingly, the magnetic structure drawn in Fig. 1 bears some similarity with that of the pure compound $CaFe_4As_3$ apart from the fact that the structure now repeats itself along the b direction as it is $k = 0$ and no longer modulated along b. Indeed, moments on sites 3 and 4 are slightly reduced while the moment on the five-coordinated site 1 is much reduced [$0.48(6)\mu_B$] like in the case of the undoped compound in the incommensurate phase. However, for the Cr-doped compound, the moment on site 2 is also reduced [$0.46(5)\mu_B$]. It is to be noted that both sites 1 and 2 with reduced magnetic moments correspond to the anchoring points between the Fe_2As_2 ribbons.

The temperature dependence of the (310) peak, obtained by integrating 74 runs from CYCLOPS is presented in the inset of Fig. 3. The extracted transition temperature of 100 K is consistent with previous magnetic susceptibility reports.[12]

To shed further light on the magnetic structure of $CaCr_{0.86}Fe_{3.14}As_3$ we have used density functional theory (DFT). The random distribution of Cr and Fe atoms on the Fe_1 special site in $CaCr_{0.86}Fe_{3.14}As_3$ results in magnetic moments at the transition metal sites that are distributed around the average values detected by the neutron diffraction measurements. *Ab-initio* calculations allow one to resolve the magnetic moments on each transition metal site and to relate them to the local distribution of Fe and Cr atoms and to their distance from the As atoms. We performed density functional calculations by using the projected augmented-wave plane-wave method as implemented in the VASP package,[18–20] with the Perdew, Burke, and Ernzerhof generalized-gradient approximation[21] to the exchange and correlation functional. The lattice vectors and atomic positions were kept fixed to their experimental values reported in Table I. In order to model the mixed occupancy by Fe and Cr on the fivefold coordinated atomic site, two supercells with $1 \times 2 \times 1$ and $1 \times 4 \times 1$ periodicity obtained by, respectively, doubling and quadrupling the primitive cell along the b axis were used. These supercells enable us to model Cr-doped $CaFe_4As_3$ with a Cr content corresponding to a $CaCr_{0.875}Fe_{3.125}As_3$ composition which closely approximates the actual composition of the sample studied. Three configurations with unique arrangements of Fe and Cr atoms on the Fe_1 special site can be produced in these supercells. The self-consistent electronic structure calculations for each of these atom arrangements converged to a magnetic configuration with the Fe atoms on adjacent Fe_2, Fe_3, and Fe_4 sites having magnetic moments parallel to each other and antiparallel to the magnetic moment of the Cr or Fe atoms occupying the Fe_1 site. The AFM configuration is lower in energy than the ferromagnetic one by 18 meV/at. The nonmagnetic configuration which reasonably approximates the paramagnetic phase is higher in energy than the AFM one by 132 meV/at. Thus, the calculations reproduced the AFM ordering observed in the experiment and shown in Fig. 1, right panel. In all configurations, the amplitude of the magnetic moments of the iron atoms on the Fe_3 sites are comprised between $2.28\mu_B$ and $2.33\mu_B$, while on the Fe_4 sites they are between $2.16\mu_B$ and $2.24\mu_B$. The magnetic moments on the Fe_2 sites have an amplitude at least $0.3\mu_B$ smaller than those on the Fe_3 and Fe_4 sites, but with a larger spread, nominally

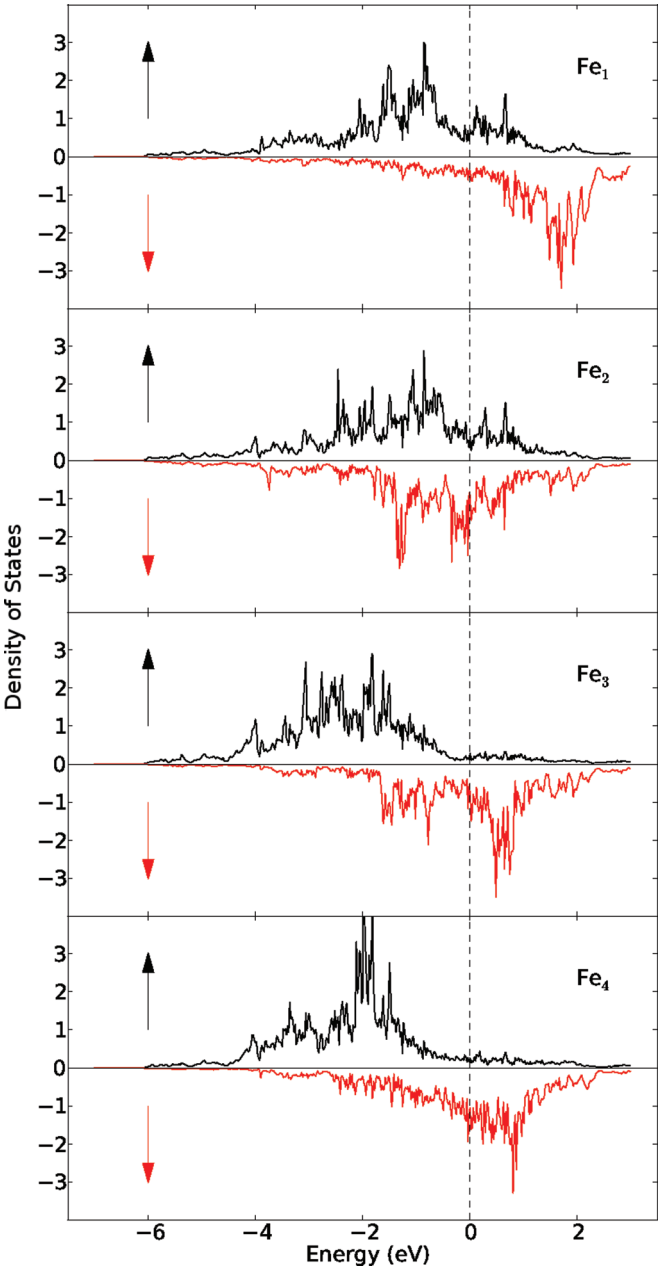

FIG. 4. (Color online) Density of states projected on the iron atomic d orbitals for all the Fe sites in the $1 \times 2 \times 1$ supercell.

between $0.78\mu_B$ and $1.93\mu_B$. Therefore, the significant reduction of the magnetic moment at the Fe_2 sites observed in the experiment is reproduced in the electronic structure calculations. We note, however, that this is not the case for the experimentally observed reduced magnetic moment on the Fe_1 site where the calculations give values of the order of $2.3\mu_B$. Figure 4 shows the projected density of states onto d orbitals of the Fe atoms at the Fe_1, Fe_2, Fe_3, and Fe_4 sites in the $1 \times 2 \times 1$ supercell. At the Fe_3 and Fe_4 sites, the spin up Fe d orbitals are fully occupied while the density of states in the spin down channel at similar energies is much smaller. Such an electronic configuration results in the large magnetic moment obtained for these sites. The total density of states, not shown here, is large at the Fermi energy which is consistent with the metallic

behavior observed in this compound. By contrast, at the Fe_2 site, the amplitude of the magnetic moment is much reduced owing to the similar density of states of spin up and spin down *d* states below the Fermi level.

In summary, we have determined the magnetic structure of $CaCr_{0.86}Fe_{3.14}As_3$ through single crystal neutron diffraction. The resulting structure is no longer incommensurate as for the undoped $CaFe_4As_3$ sample but a $k = 0$ antiferromagnet is attained instead. Moments on the sites linking the rectangular cross pattern of Fe_2As_2 ribbons are reduced. This picture is globally consistent with DFT calculations which show the lowest energy state as an AFM state with moments reduced on one of the linking sites. Further band structure calculations to determine what happens to the Fermi surface, which appeared to possess a clear nesting vector of $3\mathbf{b}^*/8$ equal to the magnetic propagation vector in the undoped sample, are required to fully understand the effect of doping. Indeed, our present results should also be placed in the general context of the iron arsenides, by discussing the relative importance of the itinerant versus the local moment description for the magnetism where the Fermi surface nesting dominates on the one hand and the exchange interactions on the other. Further experimental studies with different and smaller doping should also prove valuable in that respect.

We thank the Science and Technology Facilities Council for providing the neutron beam time at the ILL and Marek Jura for assistance with preliminary x-ray diffraction (XRD) data. The work at Argonne National Laboratory was supported by the US Department of Energy, Office of Basic Energy Sciences, under Contract No. DE-AC02-06CH11357.

[1] Y. Kamihara, T. Watanabe, M. Hirano, and H. Hosono, J. Am. Chem. Soc. **130**, 3296 (2008).
[2] R. Zhi-An, L. Wei, Y. Jie, Y. Wei, S. Xiao-Li, L. Zheng-Cai, C. Guang-Can, D. Xiao-Li, S. Li-Ling, Z. Fang *et al.*, Ch. Phys. Lett. **25**, 2215 (2008).
[3] M. Rotter, M. Tegel, and D. Johrendt, Phys. Rev. Lett. **101**, 107006 (2008).
[4] I. Todorov, D. Y. Chung, C. D. Malliakas, Q. Li, T. Bakas, A. Douvalis, G. Trimarchi, K. Gray, J. F. Mitchell, A. J. Freeman, and M. G. Kanatzidis, J. Am. Chem. Soc. **131**, 5405 (2009).
[5] Q. Huang, Y. Qiu, W. Bao, M. A. Green, J. W. Lynn, Y. C. Gasparovic, T. Wu, G. Wu, and X. H. Chen, Phys. Rev. Lett. **101**, 257003 (2008).
[6] L. L. Zhao, T. Yi, J. C. Fettinger, S. M. Kauzlarich, and E. Morosan, Phys. Rev. B **80** 020404(R) (2009).
[7] A. B. Karki, G. T. McCandless, S. Stadler, Y. M. Xiong, J. Li, J. Y. Chan, and R. Jin, Phys. Rev. B **84**, 054412 (2011).
[8] M. S. Kim, Z. P. Yin, L. L. Zhao, E. Morosan, G. Kotliar, and M. C. Aronson, Phys. Rev. B **84**, 075112 (2011).
[9] I. Nowik, I. Felner, A. B. Karki, and R. Jin, Phys. Rev. B **84** 212402 (2011).
[10] P. Manuel, L. C. Chapon, I. S. Todorov, D. Y. Chung, J. P. Castellan, S. Rosenkranz, R. Osborn, P. Toledano, and M. G. Kanatzidis, Phys. Rev. B **81** 184402 (2010).
[11] Y. Nambu, L. L. Zhao, E. Morosan, K. Kim, G. Kotliar, P. Zajdel, M. A. Green, W. Ratcliff, J. A. Rodriguez-Rivera, and C. Broholm, Phys. Rev. Lett. **106**, 037201 (2011).
[12] I. Todorov, D. Y. Chung, H. Claus, K. E. Gray, Q. Li, J. Schleuter, T. Bakas, A. P. Douvalis, M. J. Gutmann, and M. G. Kanatzidis, Chem. Mat. **22**, 4996 (2010).
[13] L. L. Zhao, S. K. Kim, G. T. McCandless, M. S. Torikachvili, P. C. Canfield, J. Y. Chan, and E. Morosan, Phys. Rev. B **84**, 104444 (2011).
[14] B. Ouladdiaf, J. Archer, J. R. Allibon, P. Decarpentrie, M-H. Lemee-Cailleau, J. Rodriguez-Carvajal, A. W. Hewatt, S. York, D. Brau, and G. J. McIntyre, J. Appl. Cryst. **44**, 392 (2011).
[15] J. Rodriguez Carvajal, Physica B **192**, 55 (1993).
[16] O. V. Kovalev, *Representations of the Crystallographic Space Groups*, 2nd ed. (Gordon and Breach Science Publishers, Switzerland, 1993).
[17] E. W. Bertaut, Acta Cryst. A **24**, 217 (1968).
[18] G. Kresse and J. Hafner, Phys. Rev. B **47**, 558 (1993).
[19] G. Kresse and J. Furthmuller, Phys. Rev. B **54**, 11169 (1996).
[20] G. Kresse and D. Joubert, Phys. Rev. B **59**, 1758 (1999).
[21] J. P. Perdew, K. Burke, and M. Ernzerhof, Phys. Rev. Lett. **77**, 3865 (1996).